Hydrodynamic Performance Analysis of a High-Speed Catamaran Based on CFD

Weijie Zhang [1], Jialin Wang [1,*], Yuting Zhang [1], Qinan Zhou [1], Xixian Ning [1], Zhongxiang Shen [1]

[1] School of Naval Architecture and Ocean Engineering, Jiangsu University of Science and Technology, Zhenjiang 212100, China.

Abstract. This research uses the CFD software STAR-CCM+ to analyze the hydrodynamic performance of a particular aluminum alloy catamaran in order to investigate the accuracy of numerical simulation forecasts utilizing CFD technology. In order to simulate the ship's motion reaction in regular waves and its still water resistance under different operating conditions, a numerical wave pool model is developed based on the Volume of Fluid (VOF) approach. The dependability of numerical calculation techniques is examined by contrasting them with model testing and establishing a correlation with the real maritime conditions of the ship's navigation posture. According to the results, the anticipated motion response in regular waves matches the ship's actual maritime navigation posture, and the CFD simulation of the catamaran's still water resistance falls within the allowable error range when compared to experimental data. As a result, CFD technology's numerical prediction accuracy satisfies engineering applications by accurately replicating the ship's condition during real navigation and offering ease of use and support for the design and optimization of comparable ships.

Keywords: Computational Fluid Dynamics; calm-water resistance; motion response.

1. Introduction

The ship's navigation performance, especially its resistance performance, is greatly impacted by the complicated and unpredictable nature of the actual sea environment, where wind and waves are the primary environmental factors acting on structures. Additionally, ships moving on waves display six degrees of freedom of motion, including pitching and rolling, which have an impact on crew member safety and equipment performance[1]. Therefore, investigating a ship's hydrodynamic performance is crucial for ship design and improvement.

The main research techniques for ship hydrodynamic performance are CFD methods, empirical formulas, theoretical calculations, and model testing. The CFD approach stands out among these due to its higher processing speeds and cheaper operating expenses. It can lower lengthy trial cycles and expensive experimental costs while enabling simulations under a variety of situations, making it a useful tool for assessing ship resistance, seakeeping performance, and maneuverability[2]. As a result, it is becoming more and more popular to analyze ship hydrodynamic performance using CFD methods. CFD techniques have already been used by researchers to examine ships' hydrodynamic performance. Chen Tao and colleagues have used the DFBI model to simulate the pitching and heaving of ships, finding distinct differences in bare hull resistance and posture during static water and self-propelled conditions. Nguyen and colleagues have employed the unsteady RANSE method to investigate the resistance and motion of KCS ships under various wave conditions, with CFD results demonstrating significant impacts of wave length on ship resistance and motion[3].

In order to forecast a particular high-speed aluminum alloy catamaran's resistance in still water and motion response when sailing in waves, this research uses the CFD program STAR-CCM+. The simulations evaluate the ship model's stability when maneuvering in waves as well as the drag at various cruising speeds. The validity of CFD numerical forecasts is investigated by contrasting them with experiments and real navigation conditions. This helps with the design and optimization of comparable vessels in future projects.

2. CFD Basic Theory and Numerical Methods

2.1 Basic Theory

The advantages of utilizing CFD software to simulate the hydrodynamic performance of ships are low cost, minimal time consumption, and efficient management of model scale effects. Predicting a ship's resistance, seakeeping performance, and maneuverability during navigation is its main function. The patterns derived from forecasts are then utilized to build and improve the ship's shape through the use of CFD techniques. The CFD solving process mainly consists of several steps as shown in Figure 1.

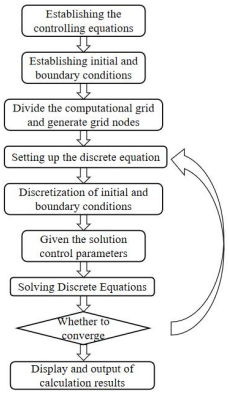

Figure. 1 CFD Workflow Diagram

2.2 Numerical Methods

The flow of an incompressible viscous fluid must satisfy the conservation of mass and momentum; thus, the selected control equations are the continuity equation (mass conservation equation) and the Navier-Stokes equations (momentum conservation equations).

(1) Continuity Equation:

$$\frac{D\rho}{Dt} + \rho div(v) = 0 \tag{1}$$

In this equation, ρ represents the fluid density, and v represents the velocity vector of the flow field.

(2) Momentum Conservation Equation:

The Navier-Stokes equations for the motion of a viscous fluid with constant viscosity are as follows:

$$\boldsymbol{\rho \frac{Dv}{Dt} = \rho F_b - gradp + div(2\mu S) + \frac{2}{3} grad(\mu divv)} \tag{2}$$

In the equations, μ represents the dynamic viscosity coefficient，F_b represents body forces, p stands for pressure, and S represents the strain rate tensor. The inertial force per unit volume of fluid is represented by the term on the left side of the equation, the mass force per unit volume by the first term on the right, the pressure gradient force acting on the fluid volume by the second term, the viscous deformation stress by the third term, and the expansion stress of the viscous body by the fourth term[4-5].

(3) Standard $k-\omega$ Model:

The standard $k-\omega$ model is widely used and relatively accurate in numerical simulation calculations, thus becoming the main turbulence model in fluid dynamics[6]. The transport equation for turbulent kinetic energy is as follows:

$$\frac{\partial(\rho k)}{\partial t}+\frac{\partial(\rho k u_i)}{\partial x_i}=\frac{\partial}{\partial x_j}\left[\left(u+\frac{u_t}{\sigma_k}\right)\frac{\partial_k}{\partial x_j}\right]+G_k+G_b-p\varepsilon-Y_M+S_k \quad (3)$$

Where k is defined as:

$$k=\frac{1}{2}u_j u_i \quad (4)$$

(4) Equation of Motion:

The motion of a ship in waves can be divided into six degrees of freedom: the movements along the x, y, and z axes are heave, sway, and surge, respectively, and the rotations around the x, y, and z axes are roll, pitch, and yaw, respectively[7]. The six degrees of freedom rigid body motion equations for ships are:

$$\begin{cases} X=m(\dot{u}-vr+wq) \\ Y=m(\dot{v}-wp+ur) \\ Z=m(\dot{w}-uq+vp) \\ K=I_x\dot{p}+(I_z-I_y)qr \\ M=I_y\dot{q}+(I_x-I_z)rp \\ N=I_z\dot{r}+(I_y-I_z)pq \end{cases} \quad (5)$$

In these equations: X represents the heaving force, Y represents the swaying force, Z represents the surging force, K represents the rolling torque, M represents the pitching torque, and N represents the yawing torque. $\dot{u}$、$\dot{v}$、$\dot{w}$ and $\dot{p}$、$\dot{q}$、$\dot{r}$, respectively, represent the corresponding linear and angular accelerations. I_x、I_y、I_z are the principal moments of inertia in the three axis directions.

3. Numerical Model and Mesh Division

3.1 Establishment of the Numerical Model

The high-speed aluminum alloy catamaran is the main focus of this project. A scaled model with a scale ratio of 1:10 was employed for numerical modeling and computing in order to improve computational performance and enable direct comparison with experimental data. Table 1 displays the principal dimensions.

Table 1. Principal Dimensions of the Ship

Item	Full-scale Parameters	Model Parameters
Scale Ratio	1：10	
Length (m)	16.9	1.69
Waterline Length (m)	15	1.5
Beam (m)	5	0.5
Depth (m)	2.1	0.21
Design Draft (m)	0.97	0.097

In Solidworks, the calculation model was constructed. Since wind resistance primarily affects the hull's superstructure, wave-making water resistance has little effect, and wind resistance makes up a small percentage of the ship's overall resistance during navigation, the deck superstructure is removed while the hull line beneath the deck remains unaltered in order to minimize the number of grids. This aluminum alloy high-speed catamaran boat's model is simplified. Figure 2 displays the simplified model, which has been exported into STAR-CCM+ and transformed into the x.t format. The following details regarding the coordinate position of the simulation model imported into STAR-CCM+ are explained in order to standardize the simulation process:

1) The origin of the simulation coordinate system is the same as the Solidworks file.
2) The X-axis points towards the bow.
3) The Y-axis points towards the port side.
4) The Z-axis is vertically upward.

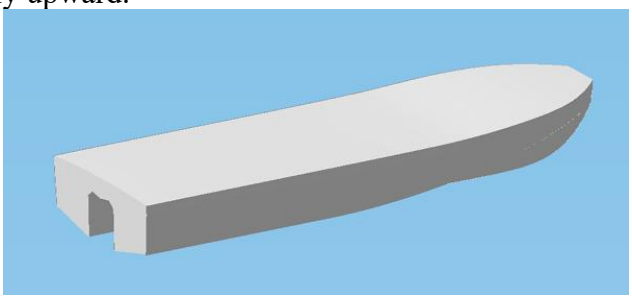

(a) General schematic of the simplified model

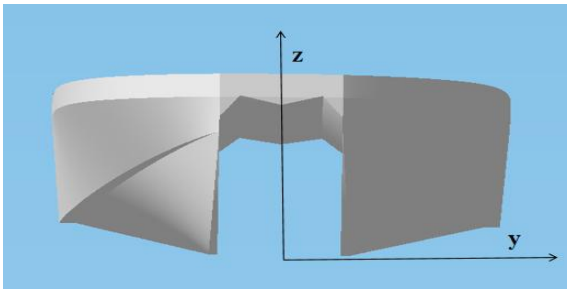

(b) Schematic view on the yz-plane

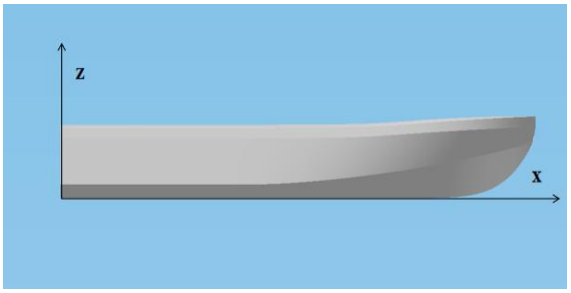

(c) Schematic view on the xz-plane

Figure. 2 Schematic Diagram of the Computational Model

3.2 Computational Domain and Mesh Division

With boundaries set sufficiently broad to reduce the impact of boundary conditions, the simulation used a rectangular computational domain of a numerical wave pool that was symmetrical about the midship section. The computational domain was divided as follows: The length of the domain was set at 1.5 times the ship length from the bow to the inlet and 2.5 times the ship length from the stern to the outlet, for a total length that was five times the ship length. The domain was 2.5 times the width of the ship on each side of the hull, making it 5 times the width of the ship; the height of the domain was 1.5 times the length of the ship above the waterline and 2.5 times the length of the ship below it. Since the fluid was moving in the negative x-direction and the domain was separated by angles at its boundaries, the top and inflow face were designated as velocity inlets, the outlet as a pressure exit boundary, and the sides as symmetrical boundaries. The plane in the center longitudinal section was designated as a symmetry plane, with the other surfaces serving as wall boundaries, due to the symmetrical nature of the aluminum alloy catamaran. To avoid affecting the outcomes, VOF wave damping boundaries were also placed at the appropriate points. The final established flow field is shown in Figure 3.

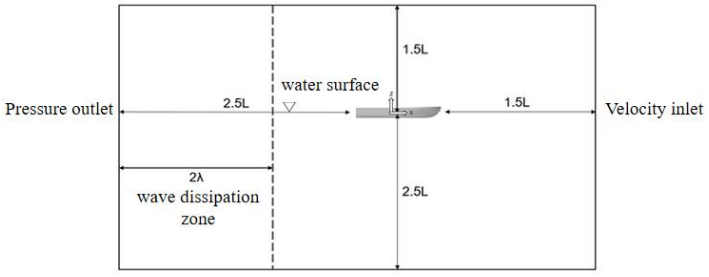

Figure. 3 Computational Domain and Boundary Conditions

The mesh of the computational domain was divided into two parts: the external flow field mesh and the densified mesh area near the ship, created using a trimmed cell mesher. The regions close to the hull and the waterline were locally densified, and the exterior flow field mesh was separated

into a structured grid. The densified grid close to the hull and the external flow field mesh are combined in this part to create the computational domain's overall mesh, which has about 1.81 million cells. Figures 4 and 5 display the domain's overall mesh and the hull's surface mesh, respectively. A trimmed boundary layer mesh was applied in five layers to the outside shell of the hull. When DFBI was first used to activate the degrees of freedom for heaving and pitching, the ship model was in a static, upright, floating condition in still water.

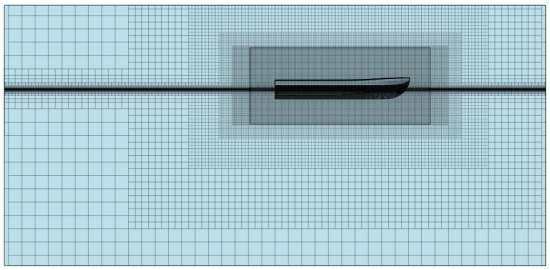

Figure. 4 Total Grid of the Computational Domain

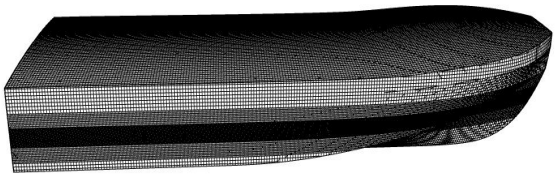

Figure. 5 Hull Surface Mesh

4. Numerical Simulation Prediction of Still Water Resistance for High-Speed Aluminum Alloy Catamaran

4.1 Numerical Simulation Results

This study examines the high-speed aluminum alloy catamaran's still water resistance at various cruising speeds. Based on the ship's actual conditions, the operational conditions for the resistance calculations were selected. With chosen circumstances at 35 knots, 36 knots, and 37 knots, the vessel's design cruising speed is 35 knots; these speeds equate to Froude numbers (Fr) of 1.485, 1.526, and 1.567, respectively. The resistance values derived from numerical simulations of the model at these speeds are displayed in Table 2. The free surface wave patterns and phase distribution diagrams from the simulations are depicted in Figures 6 and 7.

Table 2. Still Water Resistance Numerical Simulation Results

Real Ship Speed (knots)	Model Speed (m/s)	Fr	Total Resistance of Model (N)
35	5.693	1.485	37.622
36	5.856	1.526	47.639
37	6.019	1.567	57.087

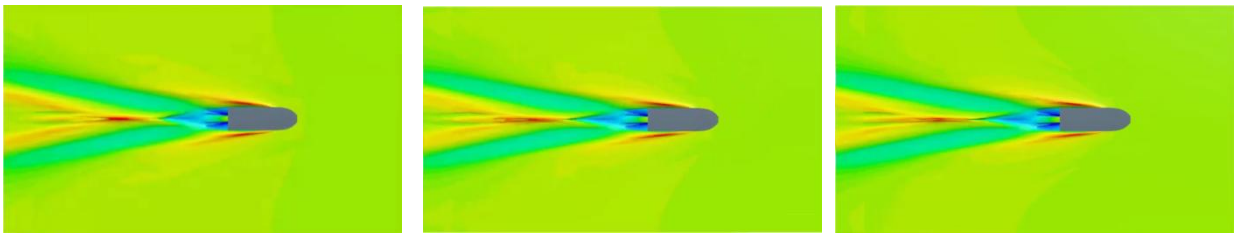

(a) V=35kn (b) V=36kn (c) V=37kn

Figure. 6 Free Surface Waveform Diagram

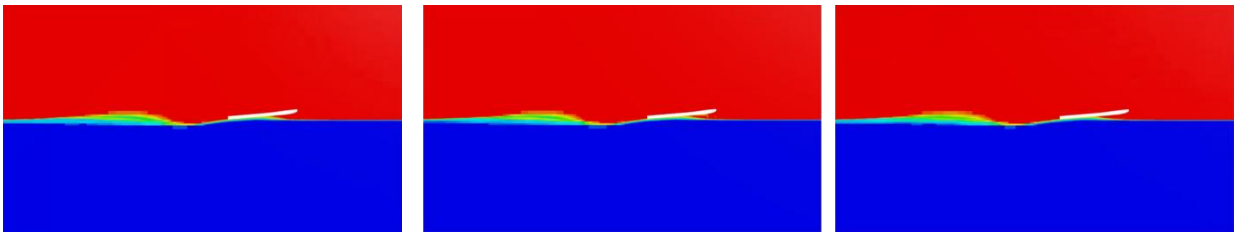

(a) V=35kn (b) V=36kn (c) V=37kn

Figure. 7 Phase Distribution Diagram

4.2 Comparison of Calculation Results

Table 3 displays the contrast between experimental values at various speeds and numerical simulation findings. During the computer calculations, it was noted that the high-speed aluminum alloy catamaran model initially created very little spray, and the wake was flat. Significant spray and a greater wake were seen at the stern as time went on and the model speed approached the predetermined cruising speed. There were also noticeable splashes on both sides and a small lifting of the bow, which is known as the bow-up phenomenon. Nevertheless, the hull maintained its stability and glided gently, performing admirably at high speeds. Experimental data indicates that the model's numerical simulation results at various speeds exhibited patterns that were comparable to the experimental values, with variations in results and errors of less than 3% falling within the acceptable error range. Thus, it is possible to forecast the resistance of the high-speed aluminum alloy catamaran using the CFD simulation program STAR-CCM+.

Table 3. Comparison of Model Calculated Values and Experimental Values

Fr	Model Speed (m/s)	Total Resistance Calculated Value (N)		
		Calculated Value	Experimental Value	Error/%
1.485	5.693	37.622	38.576	-2.53
1.526	5.856	49.639	51.233	-3.21
1.567	6.019	57.087	58.145	-1.85

5. Motion Response Analysis of a High-Speed Aluminum Alloy Catamaran in Regular Waves

5.1 Definition of Wave Heading Angle

In actual sea conditions, the design of ships must consider the seakeeping performance under complex sea states, which is particularly important in ship design. The ability of a ship to adjust to waves while navigating, including the hull's motion response and the crew's comfort and safety, is referred to as seakeeping performance. In actuality, the wave heading angle is the angle formed by the ship's advance direction and the wave advance direction. As shown in Figure 8, the primary wave heading angles are 0° for head seas, 45° for bow quartering seas, and 90° for beam seas. Two common wave heading angles—0° and 45° were chosen for consideration in this part. The motion response of the high-speed aluminum alloy catamaran at various water depths and wave heights was examined using the CFD numerical simulation program STAR-CCM+.

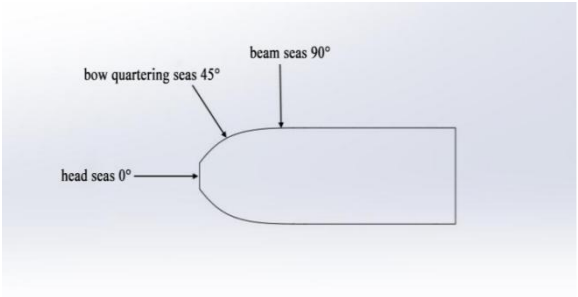

Figure. 8 Diagram of Wave Heading Angles

5.2 Motion Response Analysis at Different Water Depths

Water depths of 10 and 30 meters were chosen to examine the motion response of the high-speed aluminum alloy catamaran under six degrees of freedom at the design cruising speed of 35 knots. The wavelength to ship length ratio is set at 1 in this section. The DFBI was triggered to permit movement along the Z-axis, signifying heaving, when a wave height of 0.4 meters and a wave heading angle of 0° were selected. For the comparative study, sea depths of 10 and 30 meters were used. The same procedure was carried out again for the motion response study at various water depths while choosing a wave height of 0.8 meters and a wave heading angle of 0° . In Figure 9, specific numerical data are displayed:

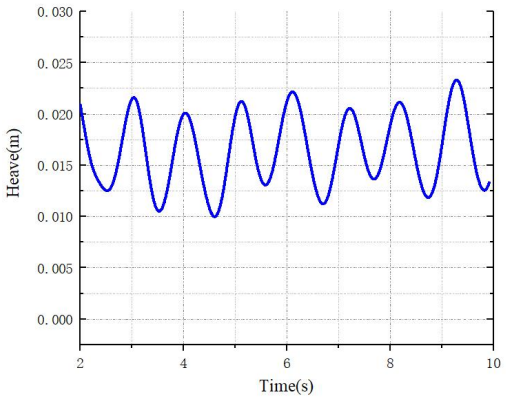

(a) 0.4m wave height-10m water depth-0° -Heaving

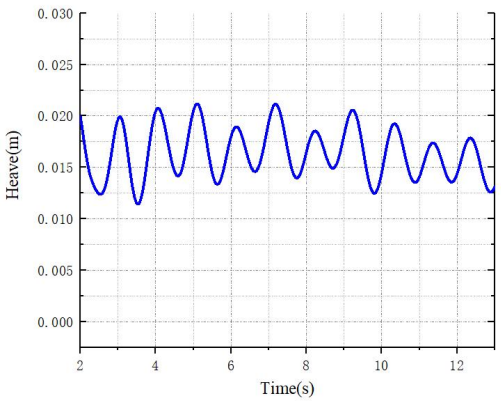

(b) 0.4m wave height-30m water depth-0° -Heaving

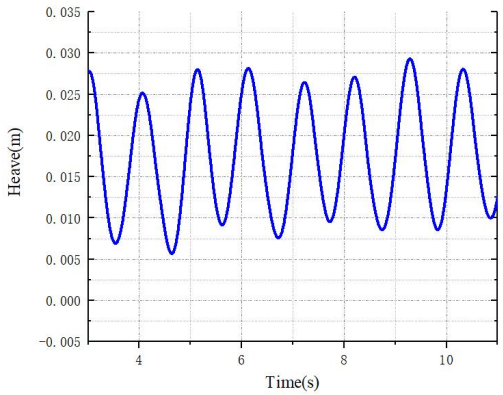

(c) 0.8m wave height-10m water depth-0° -Heaving

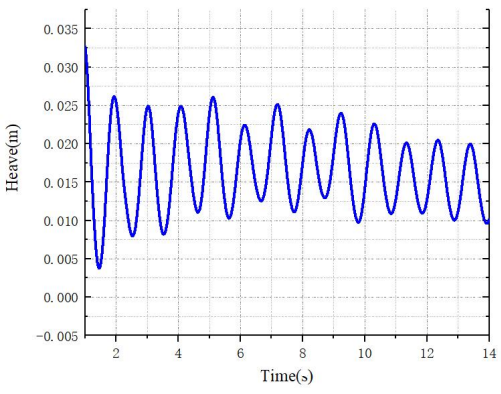

(d) 0.8m wave height-30m water depth-0° -Heaving

Figure. 9 Motion Response Analysis at Different Water Depths

Observing the heaving motion of the high-speed aluminum alloy catamaran under different water depths, the analysis of the images reveals that at a wave height of 0.4 meters with a 0° wave heading angle, compared to 30 meters, the image wave amplitude is larger at 10 meters water depth, indicating more intense heaving at shallower depths; similarly, under a wave height of 0.8 meters

with a 0° wave heading angle, the motion remains more intense at 10 meters compared to 30 meters. As a result, in comparable circumstances, the ship's motion changes with water depth: shallower waters produce more forceful motion, while deeper seas offer greater stability. This corresponds to the ship's actual sea navigating conditions. Thus, it is possible to do motion response analysis of the catamaran under study using the CFD numerical simulation program STAR-CCM+.

5.3 Motion Response Analysis at Different Wave Heights

The high-speed aluminum alloy catamaran's motion response at two distinct wave heights of 0.4 and 0.8 meters is examined in this section. To test the ship's motion reactions at different wave heights, three degrees of freedom (heaving, rolling, and pitching) were activated using DFBI at a water depth of 10 meters and a wave angle of 45 degrees. Two degrees of freedom (heaving and pitching) were engaged to conduct a comparable comparison investigation of the ship's responses at the two distinct wave heights at a water depth of 30 meters and a wave angle of 0 degrees. The numerical simulation results are displayed in Figure 10.

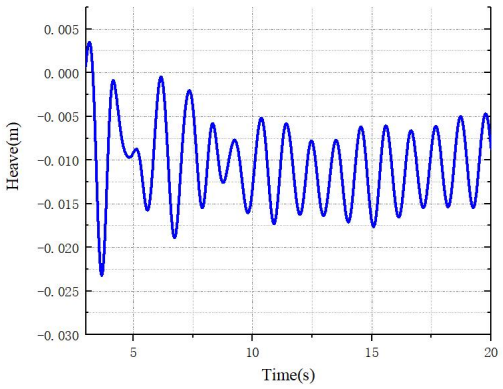

(a) 0.4m wave height-10m water depth-45° -Heaving

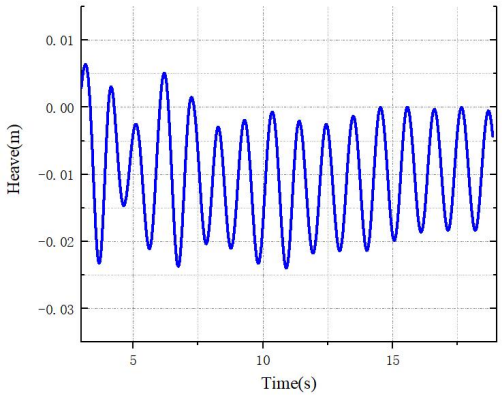

(b) 0.8m wave height-10m water depth-45° -Heaving

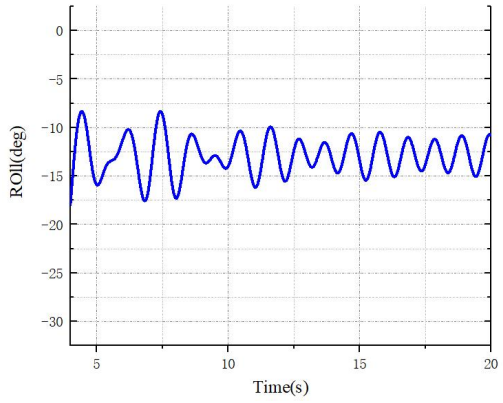

(c) 0.4m wave height-10m water depth-45° -Roll

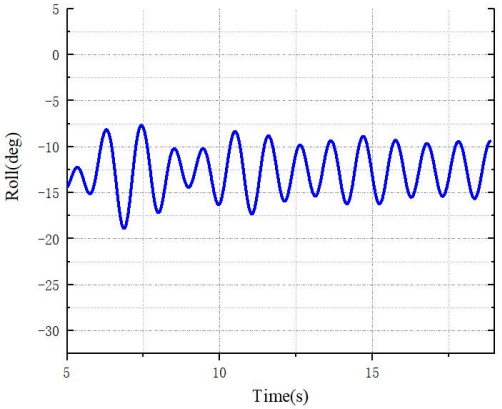

(d) 0.8m wave height-10m water depth-45° -Roll

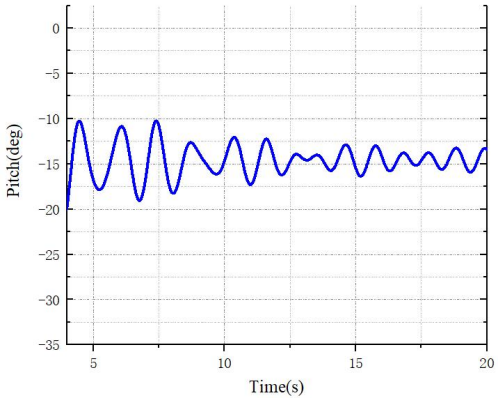

(e) 0.4m wave height-10m water depth-45° -Pitch

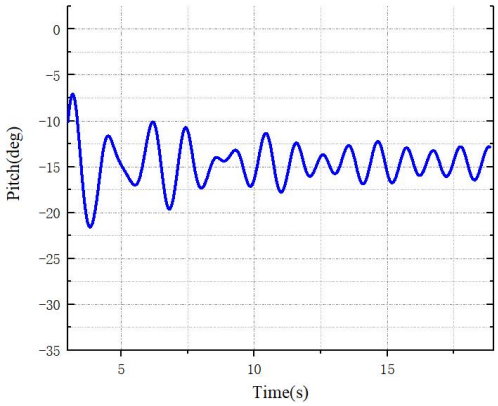

(f) 0.8m wave height-10m water depth-45° -Pitch

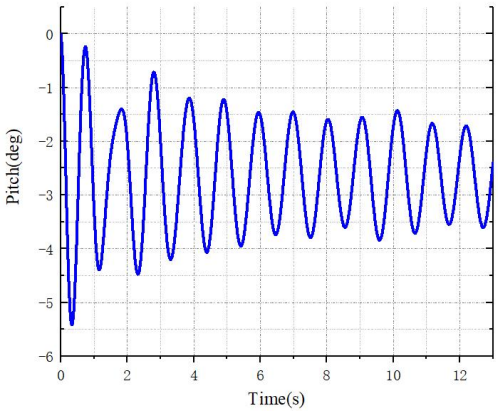

(g) 0.4m wave height-30m water depth-0° -Pitch

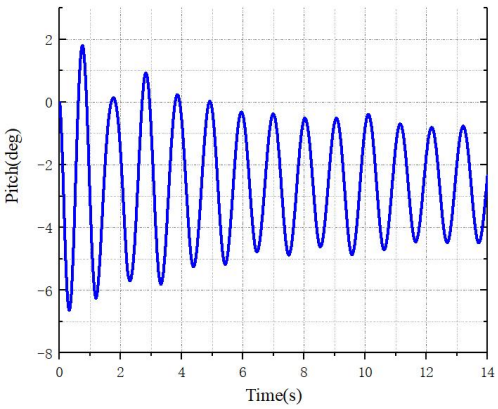

(h) 0.8m wave height-30m water depth-0° -Pitch

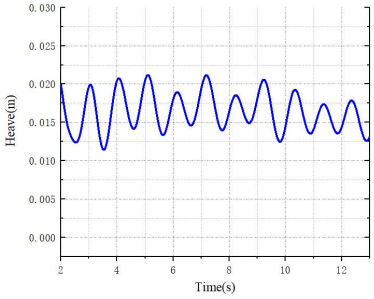

(i) 0.4m wave height-30m water depth-0° -Heave

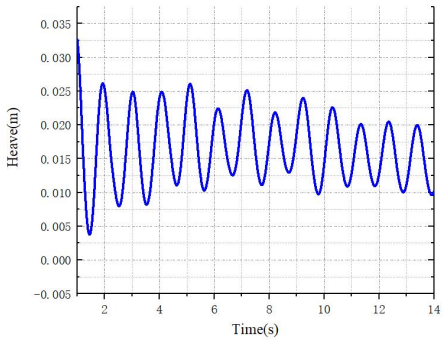

(j) 0.8m wave height-30m water depth-0° -Heave

Figure. 10 Motion Response Analysis at Different Wave Heights

Under the heaving conditions specified using DFBI, the analysis reveals that the oscillation amplitude at a wave height of 0.8 meters is much bigger than at 0.4 meters, indicating more pronounced heaving at higher wave heights. This is at a sea depth of 10 meters and a wave angle of 45 degrees. In the same way, the ship rolls more visibly at the greater wave height of 0.8 meters when the conditions are the same. We see the same pattern with pitching. Analysis of the images shows that pitching and heaving are more noticeable at 0.8 meters wave height than at 0.4 meters when the wave angle is changed to 0 degrees.

In accordance with the ship's actual maritime operating conditions, it can be determined that the high-speed aluminum alloy catamaran navigates more steadily at lower wave heights, while higher wave heights make the ship more likely to capsize. Thus, it is possible to analyze the catamaran's motion response using the CFD numerical simulation program STAR-CCM+.

The numerical simulation results are in line with the ship's actual sea navigation states when the high-speed aluminum alloy catamaran's motion response is examined using STAR-CCM+ at various wave heights and water depths. As a result, employing STAR-CCM+ makes it easier to comprehend how well a ship performs in challenging ocean conditions, which offers important information for ship design and optimization. In order to improve ship performance and safety, this research approach integrates the idea of hydrodynamic performance optimization with sophisticated simulation software. It also enables a thorough evaluation of the ship's behavior in challenging sea conditions, which is essential for improving the ship's sea adaptability and navigational stability.

6. Conclusion

In this article, the motion response and still water resistance of a high-speed aluminum alloy catamaran traveling in waves are predicted using the CFD numerical modeling program STAR-CCM+. When compared to the model test results, the numerical simulation findings for the catamaran's still water resistance fall within an acceptable error range. Furthermore, the motion response of the high-speed aluminum alloy catamaran at various wave heights and water depths as determined by numerical simulation matches the real-world maritime operational conditions of the ship. As a result, employing CFD technology to numerically forecast a ship's hydrodynamic performance satisfies engineering applications, makes it easier to comprehend how the ship will perform in challenging sea conditions, and offers convenience and support for the design and optimization of similar vessels.

References

[1] HUANG Songxing, JIAO Jialong, SUN Shuzheng, et al. Hydrodynamic performance analysis of a hybrid monohull based on computational fluid dynamics. Journal of Harbin Engineering University,2021,42(1):105-111. DOI:10.11990/jheu.201908052.

[2] Feng Jun. Research on Resistance Reduction Optimization and Seakeeping Performance of Offshore Wind Power Operation and Maintenance Catamaran based on CFD. Dalian Ocean University, 2023.DOI:10.27821/d.cnki.gdlhy.2023.000395.

[3] CHEN Yuting, XU Shihua, SHI Jiahao, et al. Hydrodynamic performance of small unmanned catamaran based on STAR-CCM+. Chinese Journal of Ship Research, 2023,18(5):73-82. DOI:10.19693/j.issn.1673-3185.02936.

[4] Wu Zixin. Analysis of Loads and Response on Marine Riser under the Combined Action of Wave and Current. Jiangsu University of Science and Technology, 2015.

[5] WANG Yafei. Study on Two Degrees of Freedom Vortex-induced Vibration of Circular Cylinder. Heilongjiang: Harbin Engineering University, 2016. DOI:10.7666/d.D01105420.

[6] Dong Ziqiang. Hydrodynamic Numerical Study of New Energy-saving Appendage behind Propeller. Jiangsu: Jiangsu University of Science and Technology, 2021.

[7] YU Xiaofeng, LIU Cong, ZHANG Xucheng, et al. Multi-objective Optimization Design of Carrier Platform of Half-rotating Impeller Tidal Turbine. Journal of Anhui University of Technology (Natural Science), 2021,38(3):282-289. DOI:10.3969/j.issn.1671-7872.2021.03.008.